

Synthesis of melt-quenched $\text{Bi}_{1.7}\text{V}_{0.3}\text{Sr}_2\text{Ca}_2\text{Cu}_3\text{O}_{10+y}$ superconducting glass-ceramics

M.E. YAKINCI, İ. AKSOY

Department of Physics, Faculty of Art and Science, İnönü University, 44069 Malatya, Turkey

M. CEYLAN

Department of Physics, Faculty of Art and Science, Firat University, Elazığ, Turkey

A glass in the BSCCO system with $\text{Bi}_{1.7}\text{V}_{0.3}\text{Sr}_2\text{Ca}_2\text{Cu}_3\text{O}_{10+y}$ nominal composition was prepared by the melt-quenching (glass) method. The suitability of the glass ceramic method has been assessed in terms of physical and electrical properties. Using an analysis developed for non-isothermal crystallization studies, information on some aspects of crystallization has been obtained. The result obtained indicated that substitution of vanadium for bismuth increased the activation energy compared to the unsubstituted BSCCO system but did not enhance the superconducting phase formation. The activation energy for crystallization of glass has been found, $E_a = 355 \text{ kJ mol}^{-1}$. The crystal structure was found to differ from that in the unsubstituted BSCCO system. Most importantly, the HT_c phase was formed by reaction between the constituent phases at lower temperatures and not directly from the glass material. The best electrical properties were obtained at $T_0 = 75 \text{ K}$ and $J_c = 12 \times 10^3 \text{ A cm}^{-2}$ at 4.2 K.

1. Introduction

Supercooled liquids (glasses) are very convenient for fundamental studies of the diffusion process and atomic rearrangement which control nucleation and crystal growth. The development of many crystal types, including metastable and stable phases, and the formation of a solid solution can be investigated under controlled conditions. Because molten glasses are good solvents for many oxides and other compounds, the effect of these, present as minor constituents, upon crystal nucleation and growth processes can be investigated. In addition, they have technological importance with respect to shaping and continuous processing if they can be processed in an appropriate viscosity range.

Alternatively, new high temperature superconducting (HT_c) oxide superconductors derived from the glass-ceramic method, obtained by melting the high-grade oxides, rapidly quenching them around room temperature and then subjecting them to a controlled heat-treatment stage, may offer many advantages and yield better properties than the ordinary solid-state ceramic technique. Many essential points for HT_c oxide superconductor materials, such as highly dense, pore-free and also homogeneous structure with strong grain connection, can be achieved. However, many attempts have been made on new HT_c oxide materials to obtain a glass form, but only the BSCCO system demonstrated full glass formation due to presence of the high glass-former oxide of Bi_2O_3 [1–3]. Although

a partly melted, devitrified and/or melt textured form of YBCO material was also produced, the full glass form was not achieved under the normal conditions. Superconductor BSCCO materials prepared by the melt-quenching method were first reported by Komatsu and co-workers, [4]. Since then other groups have prepared various compositions of superconductor samples by the glass-ceramic method [4–17]. The addition of many glass-forming agents and also other oxides were used within the BSCCO system, and glass formation and crystallization kinetics were investigated [18–21]. Although very few investigations have been performed on the vanadium substituted or doped BSCCO material, none of them has revealed the glass form of this material [22–26].

Therefore, in this investigation, vanadium was substituted for 15% Bi (according to our previous experience on the glass-ceramic BSCCO system, 15% vanadium is the optimum value for glass formation; a higher amount than 15% produces devitrified materials), and the results of crystallization kinetics and the effect of vanadium on the other physical properties are presented.

2. Experimental procedure

Appropriate amounts of reagent grade Bi_2O_3 , SrCO_3 , CaCO_3 , CuO and V_2O_5 were mixed to give a nominal composition of $\text{Bi}_{1.7}\text{V}_{0.3}\text{Sr}_2\text{Ca}_2\text{Cu}_3\text{O}_{10+y}$. The mixture was ball milled for 24 h and melted without

calcination in a covered alumina crucible at 1050 °C for 45 min in an electric furnace heated by SiC elements. The melt was then rapidly quenched between two copper plates. Approximately 1 mm thick shiny black glass sheets were obtained.

The quenched material was first examined using an automated X-ray powder diffractometer (XRD) to determine whether glass sheets were fully amorphous after quenching at room temperature. A Rigaku (system RadB) X-ray diffractometer equipped with carbon monochromator employing CuK_α radiation with the scan rate of 1°min^{-1} was used for XRD measurements. The glass sheets were then crushed and grained in an agate mortar and sieved up to $1\ \mu\text{m}$ average particle size for thermal analysis. Crystallization studies were performed under non-isothermal conditions using differential thermal analysis (DTA)-based non-isothermal kinetic theory and samples were heated using five different uniform heating rates. The DTA analyses were performed with a Shimadzu Thermal Analysis Net Work System 50 with alumina reference material. The $10^\circ\text{C min}^{-1}$ heating rate was preferred for calculations to make a comparison between the published data of the $\text{Bi}_2\text{Sr}_2\text{Ca}_2\text{Cu}_3\text{O}_{10+y}$ system. A scanning electron microscope (SEM), Jeol JSM-6100, with an energy dispersive X-ray analysis (EDX) unit (Link 10000), was used to obtain information about the surface morphology and determination of the compositions of the different phases. The electrical properties were examined by resistance ($R-T$), a.c. susceptibility and critical current density, J_c , measurements as a function of temperature in the closed-circuit helium refrigerator system (Leybold). Electrical resistance was measured from 290–10 K using the four-point configuration with conductive silver paint for contact leads at a standard current density of $10\ \text{A cm}^{-2}$. For a.c. susceptibility measurements, samples were slowly cooled from 290 K to 30 K and the data of the real components were taken. The J_c measurements were performed using the four-probe configuration with metallic indium contacts and a pulsed current system, a triangular current pulse of up to 15 A and 10 ms in length, was used to avoid ohmic heating problems at the contact points.

3. Results and discussion

3.1. Glass formation and crystallization

According to the overall degree of regularity in the atomic arrangement, the type of microstructure encountered in this investigation can easily be divided into two categories, glass (amorphous) and crystalline (solid) state. The presence of the glass from the X-ray pattern was based on the observation of a large halo at low angles on the diffraction patterns.

The XRD pattern of the glass obtained is shown in Fig. 1a. The quenched melt was found to be fully in the glass form and a broad halo (characteristic of amorphous structures), centred at $2\theta \cong 30^\circ$, was obtained. This indicates the absence of any long-range atomic arrangement (long-range order) and periodicity of a three-dimensional network in the quenched melt. No precipitated and/or undissolved Va_2O_5 material

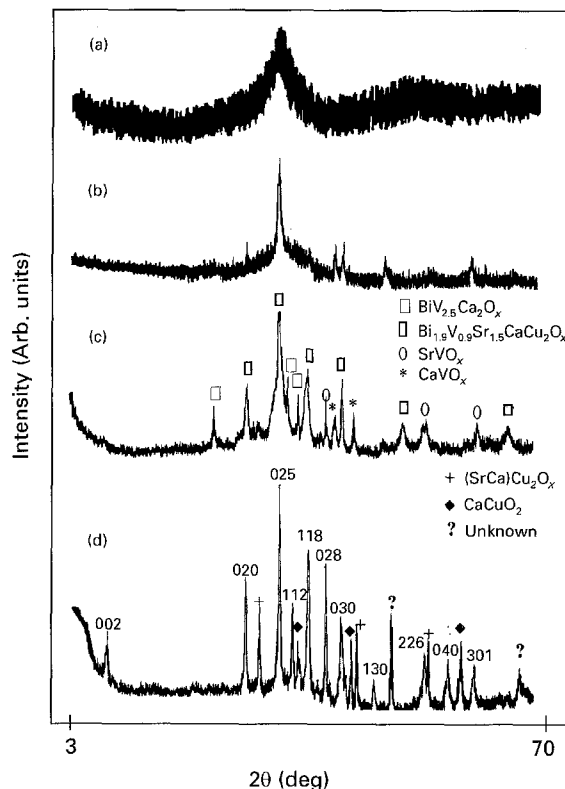


Figure 1 XRD results of the materials: (a) glass sample; (b) sample heat treated at 526 °C for 240 h; (c) sample heat treated at 750 °C for 240 h; (d) sample heat treated at 875 °C for 100 h.

TABLE I Preparation conditions and properties of the samples

Sample	Heat treatment		T_c (K)	T_o (K)	J_c (A cm^{-2}) at 4.2 K
	Temp. ($^\circ\text{C}$)	Time (h)			
1	Quenched material		—	—	—
2	400	240	—	—	—
3	525	240	—	—	—
4	750	240	—	—	—
5	800	240	45	10	5
6	855	100	70	45	177
7	855	240	80	65	8×10^3
8	875	100	80	75	12×10^3
9	875	240	75	55	7×10^3
10	880	100	60	37	125
11	880	240	40	22	10
12	885	100	Semiconductor		
13	885	240	Semiconductor		
14	890	100	Semiconductor		
15	895	100	Semiconductor		

was found anywhere in the glass material. This suggests that the appropriate viscosity range was achieved and up to 15% V in the initial mixture had no significant effect on the glassification of the system. A higher amount of vanadium in the batch (even 20% V substitution for bismuth) made glass formation difficult and devitrified material was obtained [27]. During the transformation of glass to glass-ceramic (amorphous to crystalline state) many different heat-treatment cycles were applied, and evolution of the structure was characterized step-by-step by means of XRD and SEM in conjunction with EDX. The heat-treatment temperatures, Table I, were chosen by considering the DTA results from glassy material,

TABLE II The DTA results of the material

Heating rate (°Cmin ⁻¹)	Glass transition temp., T_g (°C)	Crystallization temp., T_x (°C)	Melting temp., T_m (°C)	Glass handling temp. ($\Delta T = T_x - T_g$) (°C)
5	419	518	900	99
10	420	520	902	100
15	422	523	905	101
20	426	529	909	103
30	433	541	912	108

Table II. The XRD patterns of heat-treated material are shown in Fig. 1b–d. The results obtained showed that crystallization was not yet completed at 526 °C for 240 h heat treatment and work on the structure of the system and the phases, was difficult, Fig. 1b. The XRD pattern obtained at 750 °C for 240 h was found to differ from that of the standard unsubstituted BSCCO material, Fig. 1c. It is believed that diffusion of ions and the crystallization process are largely accelerated above 700 °C and new phases were developed at around 750 °C. The phases identified were $\text{BiV}_{2.5}\text{Ca}_2\text{O}_x$, SrVO_x , CaVO_x and $\text{Bi}_{1.9}\text{V}_{0.9}\text{Sr}_{1.5}\text{CaCu}_2\text{O}_x$. However, when the heat-treatment temperature was increased to 875 °C for 100 h, the structural differences between the samples heat treated at 750 and 875 °C were very clear, Fig. 1d. The peaks belonging to CaVO_x and SrVO_x at 750 °C had completely disappeared and many new peaks were obtained. The new phases obtained were CaCuO_2 , $(\text{SrCa})\text{Cu}_2\text{O}_x$ and also $\text{Bi}_{1.9}\text{V}_{0.9}\text{Sr}_{1.5}\text{CaCu}_2\text{O}_x$, as in the sample heat treated at 750 °C. However, the peaks at 41.08° and 68.3° were not identified; neither could they be matched to the known BSCCO system. For both samples (heat treated at 750 and 875 °C) more than ten materials, subjected to the same heat treatment, were examined; similar XRD patterns were obtained and then crystal structure analyses were performed. We strongly believe that good similarity between the XRD patterns of these identically heat-treated samples is the result of homogeneous nucleation, and then the crystallization process occurred in the glassy material during the thermal treatment stage. The X-ray powder diffraction peaks are given in Table III; the obtained and calculated peak positions are given in Tables IV and V for samples 4 and 8, respectively. Both samples have an orthorhombic unit cell, but the difference lies in the c parameter. The unit-cell parameters obtained from Tables IV and V were, $a = 0.54(5)$ nm, $b = 0.74(3)$ nm and $c = 1.06(0)$ nm, $\alpha = \beta = \gamma = 90^\circ$, for the sample heat treated at 750 °C, and $a = 0.54(1)$ nm, $b = 0.76(2)$ nm and $c = 3.01(5)$ nm, $\alpha = \beta = \gamma = 90^\circ$, for the sample heat treated at 875 °C. Calculations were based on the sharp peaks in Table III. Comparing the unit-cell parameters of both samples showed that the c -axis of sample 8 is approximately three times longer than that in the sample 4. This indicates that increased heat-treatment temperature produced a longer c -axis dimension and implies that the crystal growth largely occurs on the c -axis. It is thought from this result that the crystallization began around 525 °C, continued at

TABLE III X-ray diffraction data of the samples, where (s) indicates sharp and (w) indicates weak wide peaks in the patterns

Peak	2θ (deg)	
	Sample 4	Sample 8
1	22.20 (w)	5.85 (s)
2	26.30 (s)	23.32 (s)
3	30.15 (s)	27.70 (s)
4	31.20 (w)	29.25 (s)
5	36.00 (w)	30.10 (w)
6	37.00 (w)	31.21 (s)
7	37.80 (s)	32.40 (w)
8	39.30 (w)	33.40 (s)
9	42.80 (w)	35.30 (s)
10	45.20 (s)	35.80 (w)
11	48.15 (w)	36.45 (w)
12	54.20 (w)	37.10 (w)
13	57.70 (s)	39.05 (s)
14	–	44.80 (s)
15	–	45.30 (w)
16	–	47.70 (s)
17	–	49.30 (w)
18	–	50.70 (s)
19	–	56.10 (w)
20	–	58.10 (w)
21	–	60.60 (w)

TABLE IV Observed (selected sharp peaks from Table III) and calculated peak positions and determined indices. Maximum error is 0.08° in 2θ

Peak	Sample 4		
	2θ (obtained) (deg)	2θ (calculated) (deg)	hkl
1	26.30	26.33	112
2	30.15	30.12	103
3	33.70	33.71	122
4	37.80	37.72	104
5	45.20	45.16	124
6	57.70	57.73	026

750 °C and became stable at 875 °C. Comparing the samples heat treated at 750 and 875 °C with the $\text{Bi}_2\text{Sr}_2\text{Ca}_2\text{Cu}_3\text{O}_x$ material shows that there is no lattice matching between them. However, the structure of the 875 °C heat-treated sample was found superconducting, although it is difficult to discuss the difference between the crystal structures. However, three points are important here: firstly, we do not know whether or not bismuth sites are fully occupied by vanadium atoms. Secondly, we believe that vanadium ions would not be present only in the pentavalent form, which

TABLE V Observed (selected sharp peaks from Table III) and calculated peak positions and determined indices. Maximum error is 0.08° in 2θ

Peak	Sample 8		<i>hkl</i>
	2θ (obtained) (deg)	2θ (calculated) (deg)	
1	5.85	5.86	002
2	23.32	23.31	020
3	27.70	27.66	025
4	29.25	29.24	112
5	31.21	31.19	118
6	33.40	33.40	028
7	35.30	35.28	030
8	39.05	39.13	130
9	44.80	44.84	226
10	47.70	47.67	00
11	50.70	50.69	301

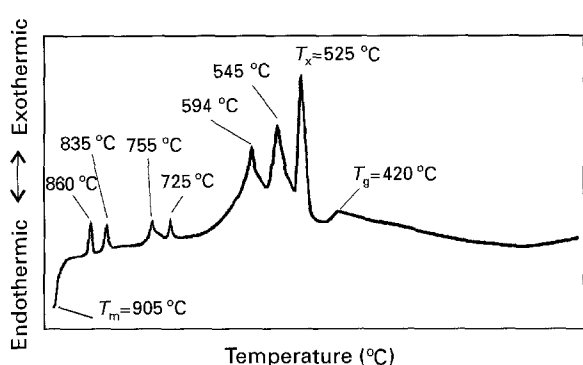


Figure 2 DTA results for the glass material. Heating condition was $10^\circ\text{C min}^{-1}$.

has $r = 0.059$ nm, but that V^{4+} ($r = 0.063$ nm), V^{3+} ($r = 0.074$ nm) or even V^{2+} ($r = 0.088$ nm) forms may also be present. Thirdly, comparing the ionic radii of vanadium ions with Bi^{3+} ($r = 0.096$ nm), bismuth has a greater atomic radius than that of the vanadium atoms. As a result of this, the bonding distance between BiO–VO layers will be increased if the bismuth sites are occupied by vanadium atoms, so it is believed that these points are very important in the crystal structure of the materials. However, according to XRD results obtained in this investigation, it was thought that at least 80% or 90% sites of the bismuth were occupied by vanadium atoms and, as a result of this, different unit cell parameters were obtained.

The DTA results from the material are shown in Fig. 2. The glass transition temperature, T_g , was found to be 420°C . The first crystallization temperature, T_x , was found at 525°C . Both results indicate that the glass-working range ($\Delta T = T_x - T_g$) is quite wide, and working with this material (handling) is not very difficult. Exothermic activities between 525 and 860°C are noticeable. The peaks at 725 and 755°C could be due to crystallization of a second ($\text{Bi}_2\text{Sr}_2\text{CaCu}_2\text{O}_x$) phase of the BSCCO system, either by reaction between the lower phases or directly from the residual glassy phase at this temperature. These two exothermic peaks were also found previously in the unsubstituted BSCCO glass material by many other

research groups [28–32]. However, peaks above 755°C are believed to be due to crystallization of the new phases, which were not found in the BSCCO material itself. This suggests that more exothermic activities occurred between 755 and 875°C , possibly as a consequence of the substitution of the vanadium, and this can be related to the structural reformation (enlargement of the c -axis). The melting point of the material was found to be 905°C , which was comparably higher than the unsubstituted BSCCO material [29–35].

The crystallization studies were made using DTA with several uniform rates, and calculations made based on the non-isothermal kinetic theory of Kissinger [36]. The basic relation was modified by Matusita and Sakka [37] and it is known as an extension of the Johnson–Mehl–Avrami kinetic model [38,39]. This relation is expressed by

$$\ln[\alpha/T_p^2] = -(E_a/RT_p) + C \quad (1)$$

where α is the heating rate, T_p the crystallization peak temperature, E_a the activation energy for crystal growth, and R the gas constant. This method was found to be useful and reliable for calculation of the activation energy and was used successfully by many other research groups for various compositions of BSCCO and also conventional glass systems [35,37]. The plot of $\ln[\alpha/(T_p)^2]$ versus $1/T_p$ gives the activation energy for crystal growth. The heating rates, glass transition and crystallization temperatures are given in Table II. A modified Kissinger plot for crystal growth in $\text{Bi}_{1.7}\text{V}_{0.3}\text{Sr}_2\text{Ca}_2\text{Cu}_3\text{O}_x$ is shown in Fig. 3. The activation energy was found to be $E_a = 355$ kJ mol^{-1} . Comparing the results obtained for different compositions of Bi–Sr–Ca–Cu–O material in earlier studies, ranging from 75 – 340 kJ mol^{-1} [18–21,40,41], clearly showed that substitution of vanadium increased the activation energy for crystallization of the BSCCO system either by changing the diffusion mechanism or by providing a long bonding distance between the BiO–VO layers.

The compositions of the glassy and crystallized materials were obtained by energy dispersive X-ray

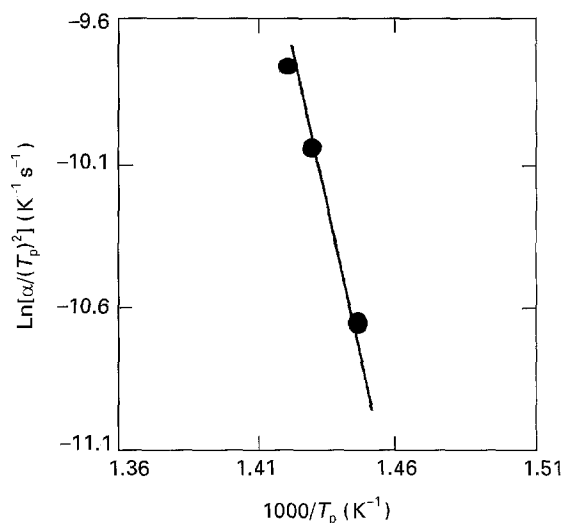


Figure 3 Modified Kissinger plot for crystal growth.

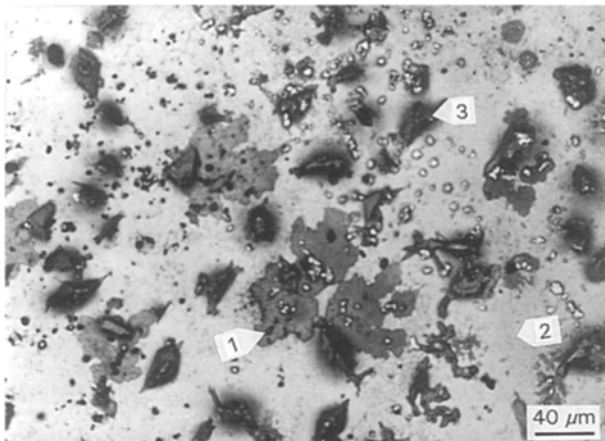


Figure 4 Scanning electron micrograph of sample heat treated at 526 °C; 1, $\text{Bi}_{1.1}\text{V}_2\text{CaO}_x$; 2, $\text{Bi}_3\text{Sr}_2\text{CaCu}_4\text{O}_x$; 3, $\text{Bi}_2\text{Ca}_2\text{CuO}_x$.

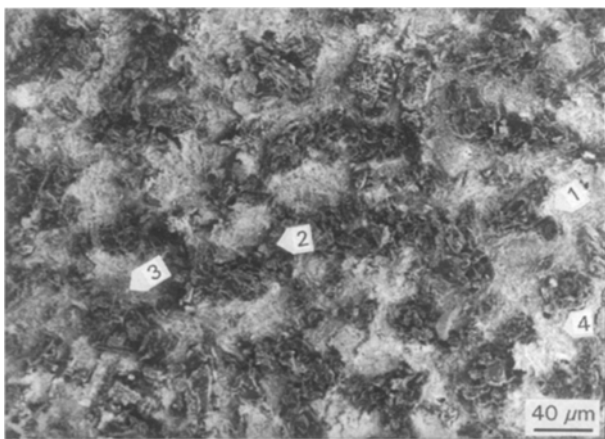


Figure 5 Scanning electron micrograph of a sample heat treated at 750 °C; 1, $\text{Bi}_{1.9}\text{V}_{0.9}\text{Sr}_{1.5}\text{Ca}_2\text{Cu}_2\text{O}_x$; 2, $(\text{CaSr})\text{Cu}_2\text{O}_x$; 3, CaVO_x ; 4, SrVO_x .

analysis. A slight stoichiometric difference for most elements was obtained after quenching. Fig. 4 shows a scanning electron micrograph of a sample heat treated at 526 °C, indicating the large nucleation centres with some small crystals of the BSCCO system; we believe that these nucleation points were initiated just above the glass transition temperature and grew rapidly below 550 °C, because SEM examination below the glass transition temperature showed no evidence of nucleation nor crystallization. The average composition of these nucleation points was found to be approximately $\text{Bi}_{1.1}\text{V}_2\text{CaO}_x$; the other zone was found to be $\text{Bi}_3\text{Sr}_2\text{CaCu}_4\text{O}_x$ phase, Fig. 4, and the small crystallized sections were found to be $\text{Bi}_2\text{Ca}_2\text{CuO}_x$. These nucleation centres did not grow into layer-like structure first; rather they grew into tightly packed flake groups at 750 °C and the melt-textured surface at around 875 °C was then obtained. At 750 °C, the $\text{Bi}_{1.9}\text{V}_{0.9}\text{Sr}_{1.5}\text{Ca}_2\text{Cu}_2\text{O}_x$ phase was found to be dominant, but newly developed $(\text{CaSr})\text{Cu}_2\text{O}_x$ solid solution, CaVO_x and SrVO_x phases were also identified, Fig. 5. However, at 875 °C, dissolution of these phases in the $\text{Bi}_2\text{Sr}_2\text{CaCu}_2\text{O}_x$ produced a partly melted surface with the general composition of $\text{Bi}_{1.5}\text{V}_{0.2}\text{Sr}_2\text{Ca}_{1.6}\text{Cu}_{2.4}\text{O}_x$ and a small amount of CaCuO_x , Fig. 6. It is thought that substitution of

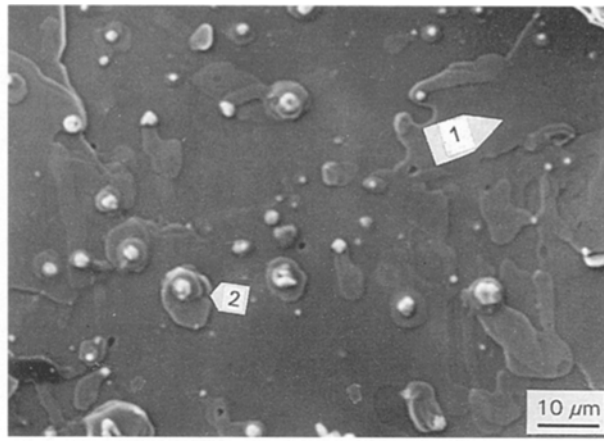


Figure 6 Scanning electron micrograph of a sample heat treated at 875 °C; 1, $\text{Bi}_{1.9}\text{V}_{0.9}\text{Sr}_{1.5}\text{Ca}_{1.6}\text{Cu}_2\text{O}_x$; 2, CaCuO_x .

vanadium is highly effective in both the nucleation and crystallization stages. We believe that particularly at temperatures between 750 and 875 °C, the ionic diffusion accelerated and later this resulted in a nearly single-phase ($\text{Bi}_{1.5}\text{V}_{0.2}\text{Sr}_2\text{Ca}_{1.6}\text{Cu}_{2.4}\text{O}_x$) of the material. As a result of this, it is considered that BSCCO glass is a good solvent for a limited amount of Va_2O_5 materials. The compositional change occurring between the initial batch ($\text{Bi}_{1.7}\text{V}_{0.3}\text{Sr}_2\text{Ca}_2\text{Cu}_3\text{O}_x$) and after the crystallization ($\text{Bi}_{1.5}\text{V}_{0.2}\text{Sr}_2\text{Ca}_{1.6}\text{Cu}_{2.4}\text{O}_x$) is probably the result of the high-temperature melting and then the long-term annealing stage, so that some of the material was evaporated. It should also be indicated that some phases obtained during the SEM–EDX investigation were not identified in the XRD traces owing to the point analysis used for EDX examinations instead of the large area analysis used in XRD examinations.

3.2. Electrical properties

The electrical properties of this material were found to be not very promising. The sample heat treated at 750 °C showed a very high resistance at room temperature (over 40 MΩ); this characteristic did not even change below 77 K. The sample heat treated between 800 and 885 °C showed metallic behaviour down to the transition temperature. However, samples heat treated between 885 and 905 °C showed semiconductor behaviour. The best electrical properties were obtained from the sample heat treated at 875 °C for 100 h. The resistance of the sample dropped linearly to 80 K and then sharp to reach zero resistance just below 75 K. This is also confirmed by the a.c. susceptibility measurements, Figs 7 and 8. Comparing the previous data obtained from unsubstituted material [16] and vanadium-substituted material, large differences are seen to exist. This suggests that the electrical behaviour is strongly dependent on the substitution of vanadium. This kind of poor electrical properties can be explained by several other factors which play critical roles in the conduction, such as, poor grain integration, intergrowth of impurity phases and destroyed phase coherence. But the result obtained in this

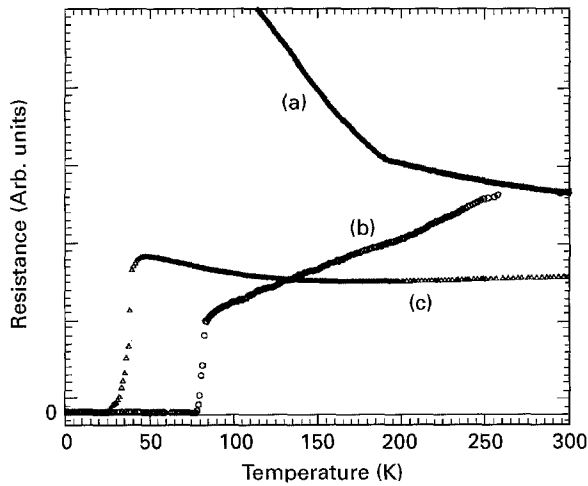


Figure 7 Resistance versus temperature graph of (a) sample 12, (b) sample 8, (c) Sample 11.

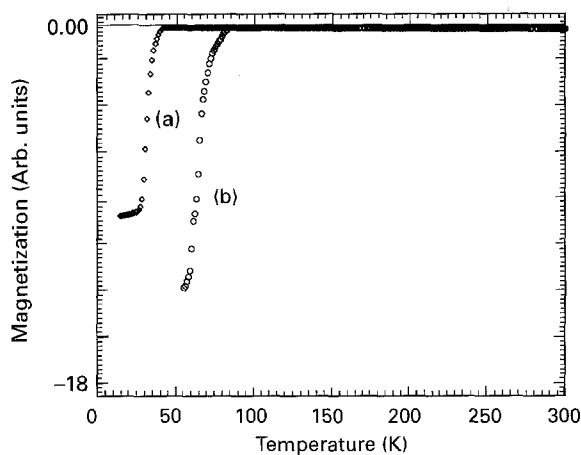


Figure 8 A.c. susceptibility measurement results: (a) sample heat treated at 880 °C for 240 h; (b) sample heat treated at 875 °C for 100 h.

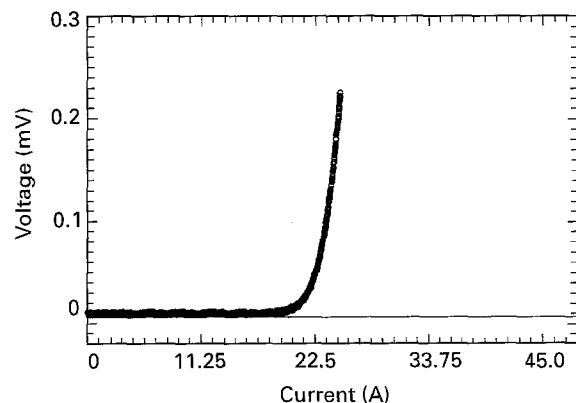


Figure 9 Critical current density measurement results of the sample heat treated at 875 °C for 100 h. $J_c = 12 \times 10^3 \text{ A cm}^{-2}$.

investigation suggests that vanadium content in the initial batch reduces the superconductive properties of the BSCCO material by destroying the electronic structure of the material, owing to the unstable valance state of the vanadium atoms. The critical current density of the same sample was found to be $12 \times 10^3 \text{ A cm}^{-2}$ at 4.2 K, Fig. 9, which is comparably lower than the $\text{Bi}_2\text{Sr}_2\text{Ca}_2\text{Cu}_3\text{O}_x$ material and suggests poor grain integration together with a damaged electronic structure.

4. Conclusion

In general, it has been discovered that vanadium in the BSCCO glass, will act as a nucleating agent and give improved nucleation. A large increase in the melting temperature, compared with the values of the unsubstituted BSCCO material, and increased activation energy in conjunction with the enhanced ionic diffusion kinetics particularly between 750 and 875 °C, were found interesting. However, this resulted in profound changes in the crystal growth and also some changes in the crystal structure, producing poor conducting facilities compared with unsubstituted BSCCO material.

Acknowledgements

We thank İnönü University Research Fund for sponsorship of this work and Professor M. J. Clark for valuable discussion of the critical current density measurement results.

References

1. P. W. McMILLAN, in "Glass-Ceramics" edited by J. P. Roberts and P. Popper (Academic Press, New York, 1979) p. 9.
2. F. M. ERNSBERGER, in "Advance in Glass Technology" edited by J. D. Mackenzie (Plenum Press, New York, 1962) p. 551.
3. R. H. DOREMUS, in "Glass Science" edited by D. R. Uhlmann (Wiley, New York, 1973) p. 24.
4. T. KOMATSU, R. SATO, K. IMAI, K. MATSUDA and T. YAMASHITA, *Jpn J. Appl. Phys.* **27** (1988) 1839.
5. R. SATO, T. KOMATSU, K. MATSUDA and T. YAMASHITA, *ibid.* **28** (1989) L583.
6. N. P. BANSAL, *Am. Ceram. Trans.* **13** (1991) p. 765.
7. Y. HIGASHIDA, H. YOKOYAMA, K. MICHISHIDA, Y. KUBO and H. YOSHIDA, *Appl. Phys. Lett.* **55** (1989) 1578.
8. Y. ABE, H. ARAKAWA, M. HOSEO and Y. HIKICHI, *Jpn J. Appl. Phys.* **29** (1989) L1929.
9. T. KOMATSU, R. SATO, K. MATSUDA and T. YAMASHITA, *Appl. Phys. Lett.* **54** (1989) 1169.
10. R. SATO, T. KOMATSU, K. MATSUDA and T. YAMASHITA, *Jpn J. Appl. Phys.* **28** (1989) 5583.
11. X. G. WANG, P. Y. HU, Z. M. HUANG and X. M. GAO, *Physica. C* **223** (1994) 327.
12. Y. NISHI, S. MORIA, S. TOKUNAGA and K. TACHIKAWA, *Mater. Sci. Lett.* **8** (1989) 247.
13. H. ZHENG, Y. HU and J. D. MACKENZIE, *Am. Ceram. Trans.* **13** (1991) p. 728.
14. M. TATSUMAGO, S. TSUBOI, N. TOHGE and T. MINAMI, *J. Appl. Phys. Lett.* **57** (1990) 195.
15. T. MATSUDA, A. SUZUKI and H. NAITO, *Supercond. Sci. Technol.* **7** (1994) 22.
16. M. E. YAKINCI, B. ULUĞ. A. ULUĞ and Z. MISIRLI, *Turkish J. Phys.* **18** (1994) 1068.
17. M. E. YAKINCI, D. HOLLAND and L. BLUNT, *Br. Ceram. Proc.* **48** (1991) 85.
18. N.P. BANSAL, *J. Appl. Phys.* **68** (1990) 1143.
19. M. E. YAKINCI, İAKSOY and A. ÖZDEŞ *Physica. C* **235-240** (1994) 959.
20. M. R. GUIRE, N.P. BANSAL and J.C. KIM, *J. Am. Ceram. Soc.* **73** (1990) 1165.
21. G. J. VALCO, V. J. KAPOOR and M. D. BIEDENBENDER, *J. Electrochem. Soc.* **136** (1989) 175.
22. T. KANAI, T. KAMO and S. MATSUDA, *Jpn J. Appl. Phys.* **28** (1989) L551.
23. P. C. W. FUNG, J. C. L. CHOW and Z. L. DU, *Supercond. Sci. Technol.* **7** (1994) 397.
24. P. C. W. FUNG, Z. C. LIN, Z. M. LIU, X. YING, Z. Z. SHENG and W. CHING, *Solid State Commun.* **75** (1990) 211.
25. X. YING, Z. Z. SHENG, F. T. CHAN, P. C. W. FUNG and K. W. WONG, *ibid.* **76** (1990) 1347.

26. *Idem, ibid.* **76** (1990) 1351.
27. M. E. YAKINCI and D. HOLLAND, unpublished data (1992).
28. H. ZHENG, Y. HU and J. D. MACKENZIE, *Appl. Phys. Lett.* **55** (1989) 1255.
29. T. KOMATSU, M. UETA, T. OHNI, R. SATO and K. J. MATSUDA, *Am. Ceram. Soc.* **75** (1992) 1864.
30. T. KOMATSU, T. TOHLI, K. MATSUDA and T. J. YAMASHITA, *J. Ceram. Soc. Jpn* **97** (1989) 251.
31. T. YAMASHITA, T. KOMATSU, K. MATSUDA and M. TAKATA, in "Proceedings of the Special Symposium on Advanced Materials", edited by T. S. Masumoto, Tokyo (Japan Institute of Metals, 1988) p. 143.
32. H. ZHENG, Y. HU and J. D. MACKENZIE, *Appl. Phys. Lett.* **55** (1989) 1255.
33. M. ONISHI, T. KOHGO, Y. CHIGUSA, M. KYOTO and M. WATANABE, *Jpn J. Appl. Phys.* **28** (1989) L2204.
34. M. ONISHI, T. KOHGO, Y. CHIGUSA, M. KYOTO, M. WATANABE and K. WATANABE, *ibid.* **29** (1990) L64.
35. S. S. OH and K. OSAMURA, *J. Mater. Sci.* **26** (1991) 4220.
36. H. E. KISSINGER, *J. Res. Natl. Bur. Stand.* **57** (1956) 217.
37. K. MATSUDA and S. J. SAKKA, *Non-Cryst. Solids* **38** (1980) 741.
38. W. A. JOHNSON and R. F. MEHL, *Trans. Am. Inst. Elect. Eng.* **135** (1939) 416.
39. M. J. AVRAMI, *Chem. Phys.* **7** (1939) 1103.
40. N. P. BANSAL, *J. Appl. Phys.* **68** (1990) 1143.
41. J. DANUSANTOSO and T. K. CHAKI, *Supercond. Sci. Technol.* **4** (1991) 509.

*Received 12 May
and accepted 20 November 1995*